An Intelligent Icons Approach for Rotor Bar Fault Detection

Petros Karvelis
Department of Applications of Information Technology in Administration and Economy,
Technological and Educational Institute of Ionian Islands
Lefkada, Greece
pkarvelis@gmail.com

George Georgoulas, Chrysostomos D. Stylios
Dept. of Informatics and Communications Technology
Technological and Educational Institute of Epirus
Arta, Greece
georgoul@teleinfom.teiep.gr, stylios@teiep.gr

Ioannis P. Tsoumas
Larges Drives R&D Department
Siemens Industry Sector - Drive Technologies
Nuremberg, Germany
ytsoumas@ieee.com

Jose Alfonso Antonino-Daviu, Vicente Climente-Alarcón
Instituto de Ingeniería Energética
Universitat Politècnica de València
Valencia, Spain
joanda@die.upv.es

***Abstract*—In this paper we propose the use of Intelligent Icons for both automatic assessment and representation of asynchronous machines' condition. The method focuses on the analysis of the start-up current for the isolation of a component that is able to pinpoint faulty signatures. The analysis is based on the application of Empirical Mode Decomposition (EMD) which acts as an adaptive filter during the start up and subsequently on the application of Symbolic Aggregate approXimation (SAX) for the transformation of the extracted component into a symbolic representation. Using this symbolic representation, an automated detection procedure can be developed that discriminates between faulty and normal conditions using an intelligent Icons approach while at the same time the information can be presented to the user in a more intuitive way.**

Keywords— Empirical Mode Decomposition, Symbolic Aggregate approXimation, Intelligent Icons, sympolic representation.

I. INTRODUCTION

Due to their low cost, robustness and minimal maintenance, asynchronous machines are incorporated in the majority of contemporary industrial drive systems. At the same time, condition monitoring of the electric drive systems leads to reduction of the maintenance costs as well as minimization of the downtime, which in turn means less production and revenue losses.

Among the different faults encountered in induction machines, rotor faults have been extensively studied even though they represent only about 5-10% [1], [2] of overall fault occurrences. One of the reasons that rotor faults are of so much interest, is because they can lead to shaft vibration and thus bearing failures and air gap eccentricity, etc.[3], while bar breakage leads to high current in adjacent bars, thus leading to potential further breakages and stator faults as well [4]. As a result, an early detection of a rotor asymmetry can be beneficial not only for the rotor but for the induction machine as a whole [3].

Motor Current Signature Analysis (MCSA) is currently the most prominent approach for rotor fault diagnosis in asynchronous machines [5],[6], primarily due to its non-invasive nature. MCSA methods usually employ the Fast Fourier Transform (FFT) of the stator current for the detection of characteristic sideband harmonic components. Among them the left sideband harmonic (LSH) has drawn the most attention since its magnitude depends on the fault severity (as well as the rotor current) and its frequency is determined by the stator supply frequency and the slip:

$$f_{LSH} = |1 - 2s| \cdot f_s \quad (1)$$

where f_s is the power supply frequency and s is the slip.

The LSH appears whenever we have any electric or magnetic asymmetry in the rotor of an asynchronous machine (either a squirrel-cage or slip-ring) [7]. However, FFT based approaches suffer from the sidelobe leakage phenomenon when trying to detect and quantify this specific component.

Moreover the analysis of the stator current during steady-state operation is complicated by the occurrence of frequencies similar to those caused by a rotor fault that can be generated by other sources such as low-frequency torsional oscillations in drive trains with gearboxes as well as voltage fluctuations [3]. Finally, the conventional FFT approach has problems when diagnosing certain specific failures such as outer cage breakages in double cage motors [8].

Due to the above reasons, a second group of methods which also relies on the analysis of the stator current but during start-up has drawn quite a lot of attention lately, [10] -[20] even though the idea of diagnosis based on transient current analysis is quite old [21],[22].

This approach has received the name of Transient Motor Current Signature Analysis (TMCSA) [13] and its underlying idea relies on tracking the characteristic evolutions of fault-related components mainly in the time-frequency (*t-f*) maps resulting from the application of suitable signal processing tools. The *t-f* signature linked to a specific fault has the advantage that it is very unlikely to be caused by another phenomenon or failure.

The application of TMCSA requires the use of signal processing tools, suited for the analysis of non-stationary quantities (such as the start-up current), that enable to obtain a time-frequency representation of the analyzed signal. These tools are known as Time-Frequency Decomposition (TFD) tools. In this context, many different TFD tools have been proposed in the electrical machines fault diagnosis area: Discrete Wavelet Transform (DWT) [12]-[15] , Continuous Wavelet Transform (CWT)[16], [17], Hilbert-Huang Transform (HHT) [18] Wigner-Ville Distribution (WVD) [19],etc. Each TFD tool provides particular advantages and drawbacks with regards to the tracking of fault-related components.

One of the main issues with the use of TMCSA methods lies either on the high dimensional nature of the extracted signatures, when the signature is represented as a time series, or the multidimensional nature of the representation when a time-frequency approach is adopted. Operators are not used to this kind of representations. Therefore automatic approaches are needed and/or more user friendly representations. In a previous study the extracted time series through the use of complex Empirical Mode Decomposition (EMD) [23] was discretized and fed to a Hidden Markov Model (HMM) [11]. One of the very few applications of a symbolic representation for fault detection in electrical machines has been presented in [24].

In this work we propose a more disciplined approach for the creation of the symbolic sequence based on Symbolic Aggregate ApproXimation (SAX) as well as a much simpler, yet effective, detection scheme for discriminating between healthy and machines with broken rotor bar(s). Moreover we present for the first time an alternative way of displaying the information to the end user using a recently developed technique for visualizing time series.

II. PREPROCESSING

Before the application of SAX some preprocessing is needed in order to isolate the part of the current signal that contains the information that is related to rotor bar faults. In this work we selected the use of EMD on one of the phase currents.

EMD lacks rigorous mathematical analysis and it decomposes the signal into a collection of Intrinsic Mode Functions (IMFs), where an IMF represents a simple oscillatory function with the following conditions that have to be satisfied: a) The number of zero crossings and the number of local extrema are equal or they differ by one and b) The local average (defined by the average of local maximum and local minimum envelops) is equal to zero.

Given a signal $x(t)$ the EMD algorithm can be summarized as follows:

1. locate all local minima and local maxima of the signal $(x(t))$
2. use the local minima and maxima to create an upper $(e_{\max}(t))$ and a lower $(e_{\min}(t))$ envelope interpolating between successive local maxima and local minima respectively
3. calculate the running mean $m(t)=\frac{e_{\min}(t)+e_{\max}(t)}{2}$
4. extract the detail by subtracting the mean from the signal $d(t)=x(t)-m(t)$.
5. repeat the whole process replacing $x(t)$ with $m(t)$ until the final residual becomes a constant value, a monotonic function or a function with only one extremum from which no more IMFs can be extracted (or a user specific number of IMFs has been extracted – application dependent).

In practice, step 4 may not produce a valid IMF and sifting needs to take place, which implies the iteration of steps 1 to 4 upon the detail $d(t)$ until a specific criterion is met [23], [25].

As it was proven in [20], the faulty component is mainly contained in the second IMF as it can be seen in Fig. 1 (extracted using the EMD toolbox [26]), where the second IMF for the case of a healthy machine and a machine with one and two broken bars is depicted. Note: all currents are normalized to have maximum amplitude equal to one. After the extraction of this specific IMF, SAX is applied.

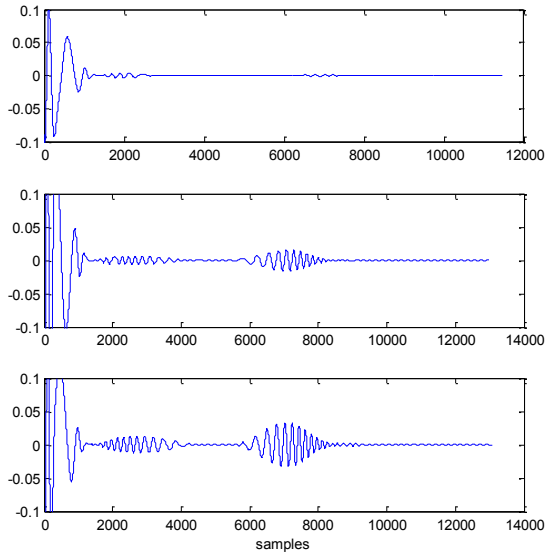

Fig. 1: The second IMF of the start-up current for a) healthy machine, b) a machine with one broken bar and c) a machine with two broken bars

III. SYMBOLIC AGGREGATE APPROXIMATION (SAX)

The SAX representation has been successfully used in a variety of applications including indexing, classification, clustering [27], motif discovery [28], rule discovery, [29], visualization [30] and anomaly detection [31].

SAX takes as input a time series (signal) of arbitrary length N and reduces it to a string of length w, ($w << N$) using a predefined alphabet. The alphabet length A is an integer, where $A > 2$. This string then can be used to construct a table of frequencies of sub words. This table can be represented as an image or as an icon of the signal. For long time series, we slide a window across it, and obtain the final SAX word [35]. The following subsections describe in more detail each step of SAX and its application for the creation of Intelligent Icons representation.

A. Piecewise Aggregate Approximation

The SAX representation is created by taking a real valued signal and dividing it into equal sized sections. After that the mean value of each section is calculated. By substituting each section with its mean, a reduced dimensionality Piecewise Aggregate Approximation (PAA) of the data is obtained. Then the PAA representation is converted into a discrete string. The PAA representation of a time series has been shown to rival more sophisticated dimensionality reduction techniques [32].

A time series S of length N can be represented in a w-dimensional space by a vector $\overline{S} = \overline{s_1}, \ldots$. The i-th element of S is calculated by the following equation:

$$\overline{s_i} = \frac{w}{N} \sum_{j=\frac{w}{N}(i-1)+1}^{\frac{w}{N}i} s_j \qquad (2)$$

Thus, in order to reduce the time series from N dimensions to w dimensions, the data is divided into w equal sized windows. The mean value of the data falling within a frame is calculated and a vector of these values becomes the data-reduced representation. It must be mentioned that prior to the computation of the PAA the section of the time series is normalized in order to have zero mean and standard deviation equal to one. An example of the PAA of a time series is shown in Fig. 2.

B. Discretization

After the times series S has been transformed to its PAA approximation we obtain a discrete representation. Having normalized the time series our new time series will approximately follow a Gaussian distribution and we can simply determine the "breakpoints" that will produce equal-sized areas under a Gaussian curve [33]. After the computation of the breakpoints, discretization takes place:

- all PAA coefficients that are below the smallest breakpoint are mapped to the symbol "a",
- all coefficients greater than or equal to the smallest breakpoint and less than the second smallest breakpoint are mapped to the symbol "b",
- etc.

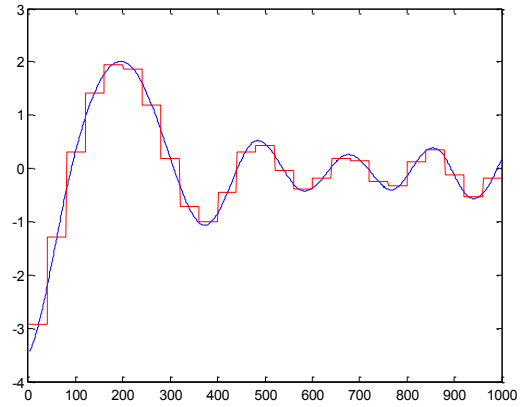

Fig. 2: The PAA representation of a normalized time series of an original length of N=1000 using w=25.

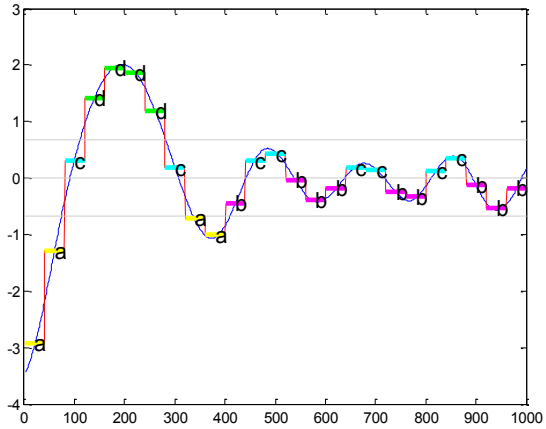

Fig. 3: The discretization of the time series depicted in Fig. 2 using an alphabet of length 4.

Fig. 3 depicts the discretization process of the signal displayed in Fig. 2, after the PAA stage. In this example the parameters are $N = 100$, $w = 25$ and $A = 4$, the time series is mapped to the word SAX_S = aacddddcaabccbbbccbbccbbb.

C. Intelligent Icon Computation

After we have computed the SAX representation our goal is to transform this word into an Intelligent Icon. The first attempt, to map a sequence into an icon would be to divide the bitmap into four quadrants and count the frequency of each of the four possible base pairs. If we want to generalize this we can count the frequencies of specific sub words of length l. For $l = 1$ words, frequencies are the counts of the symbols used. For words of length $l = 2$ the frequencies are the counts of sub words of size 2 (e.g. "aa", "ab", "ac", etc.). For example the icon of the word SAX_S = aacddddcaabccbbbccbbccbbb is shown in Fig. 4.

a:4	b:9
c:8	d:4

a

aa:2	ab:0	ba:0	bb:5
ac:1	ad:0	bc:3	bd:0
ca:1	cb:3	da:0	db:0
cc:3	cd:0	dc:1	dd:3

b

Fig. 4: The Icons for the SAX word $SAX_S = \text{aacddddcaabccbbbccbbccbbb}$. (a) The frequencies and the sub words of level $l = 1$ and (b) the same for $l = 2$.

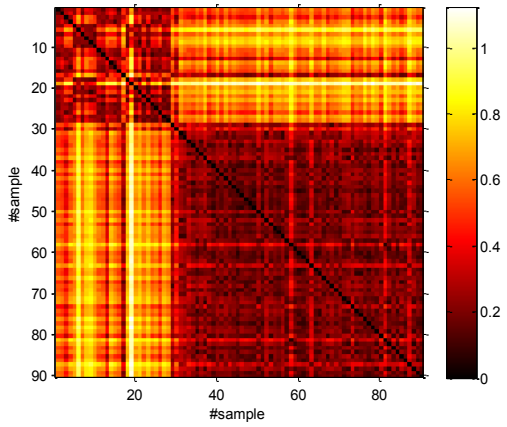

Fig. 5: The distance matrix between each intelligent icon for the 90 signals.

First we assign to each letter of the alphabet a unique value k:

$$a = 0, b = 1, c = 2, d = 3 \ . \tag{3}$$

Each word has an index for the location of each symbol in the table of the icon. For clarity we can show them explicitly as subscripts. For example, the first word with $l = 2$ extracted from SAX_S is a_0a_1. In this example $k_0 = a$, $k_1 = a$. Then in order to map a sub word to the icon we can use the following equations to find its row and column values:

$$col = \sum_{n=0}^{l-1} (k_n \cdot 2^{l-n-1}) \bmod 2^{l-n} \ , \tag{4}$$

$$row = \sum_{n=0}^{l-1} (k_n div 2) \cdot 2^{l-n-1} \ . \tag{5}$$

Intelligent Icons can be used to display time series in a more compact form or be used as feature vectors for classification/detection purposes. In this study they were used in both forms.

IV. Results

A. Dataset

In order to test our approach, start-up currents from a healthy and from a machine with one and two broken rotor bars were examined. The start-up currents were selected using three current transducers resulting in three recordings for each experiment. We ran 10 start ups for each one of the three conditions. Therefore we had 30 recordings for the healthy condition and 60 for the faulty condition (30 recordings with one broken bar and another 30 recordings with two broken bars).

B. Classification

Having presented the new representation of time series, we can now define a distance measure on it. By far the most common distance measure for time series is the Euclidean distance. Given two time series f_1 and f_2 of the same length N, and their icons I_{f_1}, I_{f_2} we can define their Euclidean distance as:

$$D(I_{f_1}, I_{f_2}) = \sqrt{\sum_{i=1}^{8}\sum_{j=1}^{8} (I_{f_1}(i,j) - I_{f_2}(i,j))^2} \tag{6}$$

Fig. 5 displays the distance between each icon and the rest of the icons of the data set. The first 30 samples belong to the healthy machine and the rest 60 belong to the faulty machine (keep in mind that in this study we have grouped together the two faulty conditions approaching the problem from a fault detection approach rather than a diagnosis one). Notice the two distinct blocks that are shown in Fig. 5; their presence indicates the existence of two classes.

Using a nearest neighbor (NN) classifier, the distance defined by Eq. 6 and employing a leave-one-out classification scheme we have perfect detection of a faulty situation without false alarms. In other words each time we used 89 of the recordings for creating the training set of the NN classifier and the case left out was used for testing the detection accuracy.

The success of the approach in discriminating between faulty and healthy machines can be further elaborated using Multi-Dimensional Scaling (MDS) [34] in order to display the produced representation in the two dimensional space. MDS requires the distance matrix computed by Eq. (6). Fig. 6, displays the MDS projection on the two dimensional space along with the boundary created using as inputs the coordinates of the space as inputs to a nearest neighbor classifier. As one can easily observe the icons of the signals are separable even at this lower dimensional space. Therefore the task can be even easier in the original higher dimensional feature space.

C. Intelligent Icons

An interesting feature of the application of our method is the fact that similar signals (signals of the same class) will have similar icons. As one can observe from Fig. 7 the icon of signal #20 is similar to the icon of signal #27. As one can observe by Fig. 7, this is also true for their signals. Both cases correspond

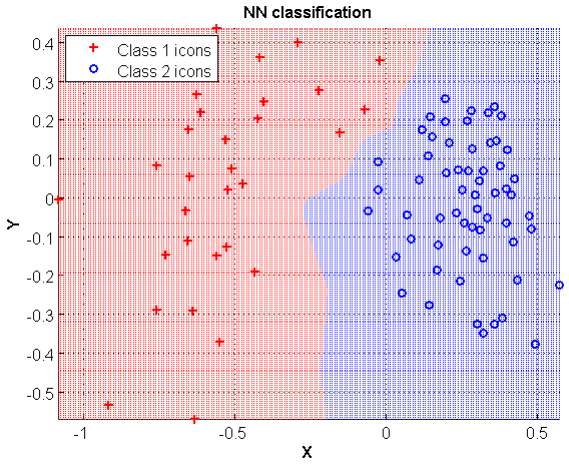

Fig. 6: Multidimensional Scaling and classification boundary using k-NN classification rule (k=1).

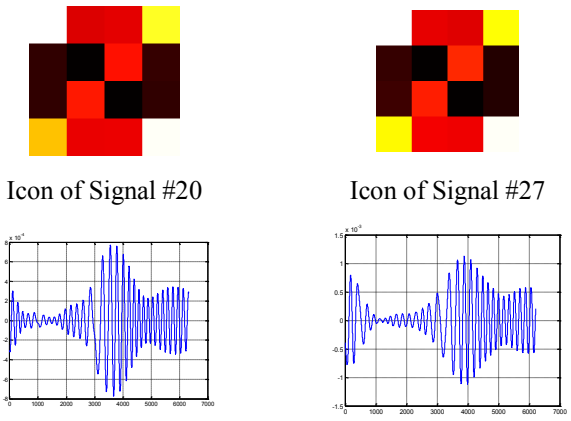

Fig. 7: Two visually similar Icons and their signals for the case of a healthy machine.

to recordings produced from a healthy machine. This is also the case for signals produced from a machine with broken bar(s). In Fig. 8 the icons of the signals #32 and #36 are shown along with their icons, corresponding to a machine with one broken bar.

V. Conclusions & Discussion

This study presents for the first time the application of SAX and the Intelligent Icons technique for the detection of broken rotor bars in asynchronous machines. The results indicate that the approach can easily discriminate between healthy and asynchronous machines with broken rotor bars.

The main drawback of the approach is due to one of its advantages when considered in other application domains: its scale invariance. In other words our approach in its current form cannot be used for the diagnosis of the severity of the problem. This is an open area for research for us, as well as the use of SAX with multidimensional data such as those produced by the UWT.

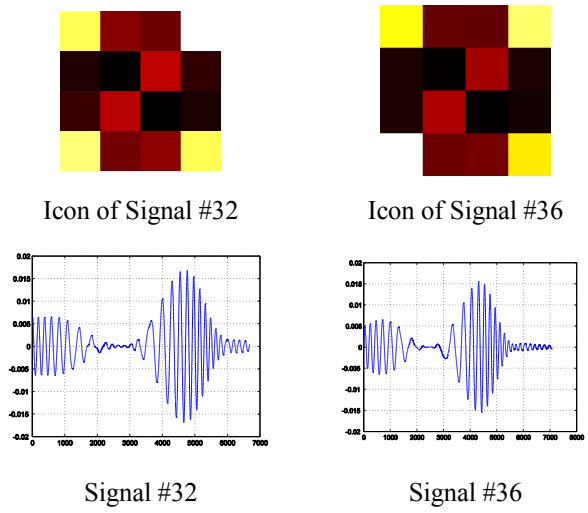

Fig. 8: Two similar Icons and their signals for the case of a machine with one broken bar.

Even though SAX is an algorithm which needs light configuration it still has some parameters that need to be defined by the user. First the size of the sliding window, second the number of equal sized sections in which to divide, third the size of the alphabet and finally the length of the sub words. A good choice for the sliding window should reflect the natural scale at which the events occur in the time series [35]. Thus in our case we have set the value of the sliding window empirically. In our study we conducted many experiments varying the number of equal sized sections, length of the alphabet and length of sub words. The SAX related parameters were selected based on visual inspection of the MDS representation; a set of parameters capable of creating a visually separable result for the two classes was acquired without further attempt to optimize the results. Specifically, we used the following values for the parameters: window size $N = 2000$, number of segments $w = 100$, size of alphabet $A = 4$ and size of words $l = 2$. In future work we will try to automate this process and also further investigate combination of parameters to achieve discrimination also between the faulty classes, i.e. discriminate among different number of broken bars. Finally we must note that the approach is general and thus it can be also used for the discrimination of other types of faults (eccentricity, short circuit faults etc.) as well as simultaneous faults, during the start up.

VI. Appendix

Rated characteristics of the 1.1 kW motor: Star connection, rated voltage (U_n): 400V, rated power (P_n): 1.1 kW, 2 pair of poles, primary rated current ($I1_n$): 2.7A, rated speed (n_n): 1410 rpm and rated slip (s_n): 0.06. The number of rotor bars is 28.

References

[1] A. H. Bonnett and G. C. Soukup, "Rotor failures in squirrel cage induction motors," *IEEE Trans. Ind. Appl.*, vol. IA-22, no. 6, pp. 1165–1173, Nov./Dec. 1986.

[2] A. H. Bonnett and C. Yung, "Increased efficiency versus increased reliability," *IEEE Ind. Appl. Mag.*, vol. 14, no. 1, pp. 29-36, 2008.

[3] P. Zhang, Y. Du, T. G. Habetler, and B. Lu, "A Survey of Condition Monitoring and Protection Methods for Medium Voltage Induction Motors," *IEEE Trans. Energy Convers*., vol. 47, no. 1, pp. 34–46, Jan. 2011

[4] A. Bellini, F. Filippetti, C. Tassoni, and G. Capolino, "Advances in diagnostic techniques for induction machines", *IEEE Trans. Ind. Electron*, vol. 55, no. 12, pp. 4109–4126, 2008.

[5] M. A. Awadallah and M. M. Morcos, "Application of AI tools in fault diagnosis of electrical machines and drives-an overview," *IEEE Trans. Energy Convers*., vol. 18, no. 2, pp. 245–251, Jun. 2003.

[6] M. Benbouzid, "A review of induction motors signature analysis as a medium for faults detection," *IEEE Trans. Ind. Electron.*, vol. 47, no. 5, pp. 984–993, Oct. 2000.

[7] K. Kovacs, and I. Racz, *Transient phenomena in AC machines* (in German), vol. 1, Hungarian Academy of Sciences Publishing, Budapest, 1959.

[8] J. Antonino-Daviu, M. Riera-Guasp, J. Pons-Llinares, J. Park, S.B. Lee, J. Yoo and C. Kral, "Detection of Broken Outer-Cage Bars for Double-Cage Induction Motors Under the Startup Transient," *IEEE Trans. Ind. Appl*, vol. 48, no.5, pp. 1539-1548, Sept/Oct 2012.

[9] Z. Zhang, Z. Ren, and W. Huang, "A novel detection method of motor broken rotor bars based on wavelet ridge," *IEEE Trans. Energy Convers.*, vol. 18, pp. 417-423, 2003.

[10] G. Georgoulas, M. O. Mustafa, I. P. Tsoumas, J. A. Antonino-Daviu, V. Climente-Alarcon, C. D. Stylios, and G. Nikolakopoulos, "Principal Component Analysis of the Start-up Transient and Hidden Markov Modeling for Broken Rotor Bar Fault Diagnosis in Asynchronous Machines," *Expert Systems with Applications,* vol. 40, no. 19, pp. 7024–7033, 2013.

[11] G. Georgoulas, I. Tsoumas, E. Mitronikas, C. D. Stylios, and A. Safacas, "Rotor fault diagnosis in asynchronous machines via analysis of the start-up transient into intrinsic mode functions," in proc. *XXth IEEE International Conference on Electrical Machines* (*ICEM*), Marseille, France, pp. 2498-2504, 2012.

[12] J. A. Antonino-Daviu, M. Riera-Guasp, J. Roger-Folch, and M. Palomares, "Validation of a new method for the diagnosis of rotor bar failures via wavelet transform in industrial induction machines", *IEEE Trans. Ind. Appl.*, vol. 42, no. 4, pp. 990-996, 2006.

[13] M. Riera-Guasp, J. A. Antonino-Daviu, M. Pineda-Sanchez, R. Puche-Panadero, and J. Perez-Cruz, "A general approach for the transient detection of slip-dependent fault components based on the discrete wavelet transform," *IEEE Trans. Ind. Electron*., vol. 55, no. 12, pp. 4167–4180, Dec. 2008.

[14] H. Douglas, P. Pillay, A. Ziarani, "A new algorithm for transient motor current signature analysis using wavelets", *IEEE Trans. Ind. Appl.*, vol. 40, no. 5, pp. 1361-1368, 2004.

[15] M. Riera-Guasp, J. A. Antonino-Daviu, J. Roger-Folch, and M. P. M. Palomares, "The use of the wavelet approximation signal as a tool for the diagnosis of rotor bar failures," IEEE Trans. Ind. Appl., vol. 44, no. 3, pp. 716-726, May/Jun. 2008.

[16] F. Briz, M. W. Degner, P. Garcia, and D. Bragado, "Broken rotor bar detection in line-fed induction machines using complex wavelet analysis of startup transients," IEEE Trans. Ind. Appl., vol. 44, no. 3, pp. 760-768, May/Jun. 2008.

[17] R. Supangat, N. Ertugrul, W. L. Soong, D. A. Gray, C. Hansen, and J. Grieger, "Broken Rotor Bar Fault Detection in Induction Motors Using Starting Current Analysis," *IEEE 11th European Conference on Power Electronics and Applications,* Dresden, Germany, Sept. 2005.

[18] J. A. Antonino-Daviu, P. J. Rodriguez, M. Riera-Guasp, A. Arkkio, A., J. Roger-Folch, and R. B. Perez, "Transient detection of eccentricity-related components in induction motors through the Hilbert–Huang Transform," *Energy Conversion and Management*, vol. *50, no.* 7, pp. 1810-1820, 2009.

[19] V. Climente-Alarcon, J.A. Antonino-Daviu, M. Riera-Guasp, R. Puche-Panadero, and L. Escobar, L. "Application of the Wigner–Ville distribution for the detection of rotor asymmetries and eccentricity through high-order harmonics," *Electric Power Systems Research*, vol. 91, pp. 28-36, 2012.

[20] J.A. Antonino-Daviu, M. Riera-Guasp, M. Pineda-Sanchez,and R.B. Perez, "A Critical Comparison Between DWT and Hilbert–Huang-Based Methods for the Diagnosis of Rotor Bar Failures in Induction Machines," *IEEE Trans. Ind. Appl.*, vol. 45, no. 5, pp 1794-1803, Sept/Oct. 2009.

[21] S. Elder, J. F. Watson, and W. T. Thomson, "Fault detection in induction motors as a result of transient analysis," in *Proc. IEEE 4th Int. Conf. Elect. Mach. Drives*, London, U.K., pp. 182–186, 1989.

[22] R. Burnett, J. Watson, and S. Elder, "The application of modern signal processing techniques to rotor fault detection and location within three phase induction motors", *Signal Process.*, vol. 49, no. 1, pp. 426-431, 1996.

[23] N. E. Huang, Z. Shen, S. R. Long, M. L.Wu, H. H. Shih, Q. Zheng, N. C. Yen, C. C. Tung, and H. H. Liu, "The empirical mode decomposition and Hilbert spectrum for nonlinear and non-stationary time series analysis," in *Proc. of the Royal Society London A*, vol. 454, pp. 903–995, 1998.

[24] S. Chakraborty, E. Keller, A. Ray, and J. Mayer, Detection and estimation of demagnetization faults in permanent magnet synchronous motors. *Electric Power Systems Research*, vol. 96, pp. 225-236, 2013.

[25] G. Rilling, P. Flandrin, and P. Gonçalvès, "On empirical mode decomposition and its algorithms" in *Proc. of 6th IEEE-EURASIP Workshop on Nonlinear Signal and Image Processing* (NSIP '03), Grado, Italy, June 2003.

[26] The EMD toolbox <http://perso.ens-lyon.fr/patrick.flandrin/emd.html> (last accessed 08.29.2012).

[27] Lin, J., Keogh, E., Lonardi, S. & Chiu, B. (2003) A Symbolic Representation of Time Series, with Implications for Streaming Algorithms. In proceedings of the eighth ACM SIGMOD Workshop on Research Issues in Data Mining and Knowledge Discovery.

[28] Chiu, B., Keogh, E., & Lonardi, S. (2003). Probabilistic Discovery of Time Series Motifs. In the 9th ACM SIGKDD International Conference on Knowledge Discovery and Data Mining, pp. 493-498.

[29] Silvent, A. S., Carbay, C., Carry, P. Y. & Dojat, M. (2003). *Data, Information and Knowledge for Medical Scenario Construction*. In proceedings of the Intelligent Data Analysis In Medicine and Pharmacology Workshop. Protaras, Cyprus.

[30] Lin, J., Keogh, E., Lonardi, S., Lankford, J.P. & Nystrom, D.M. (2004). Visually Mining and Monitoring Massive Time Series. In proceedings of the tenth ACM SIGKDD International Conference on Knowledge Discovery and Data Mining.

[31] Keogh, E., Lonardi, S., & Ratanamahatana, C. (2004). Towards Parameter-Free Data Mining. In proceedings of the tenth ACM SIGKDD International Conference on Knowledge Discovery and Data Mining.

[32] Keogh, E., Chakrabarti, K., Pazzani, M. & Mehrotra, S. (2001). Locally Adaptive Dimensionality Reduction for Indexing Large Time Series Databases. In proceedings of ACM SIGMOD Conference on Management of Data. Santa Barbara, CA, May 21-24. pp 151-162.

[33] Larsen, R. J. & Marx, M. L. (1986). An Introduction to Mathematical Statistics and Its Applications. Prentice Hall, Englewood, Cliffs, N.J. 2nd Edition.

[34] Borg, I., Groenen, P. (2005). Modern Multidimensional Scaling: theory and applications (2nd ed.). New York: Springer-Verlag. pp. 207–212. ISBN 0-387-94845-7.

[35] Kumar, N., Lolla N., Keogh, E., Lonardi, S. , Ratanamahatana, C. A. and Wei, L. (2005). Time-series Bitmaps: A Practical Visualization Tool for working with Large Time Series Databases . In proceedings of SIAM International Conference on Data Mining (SDM '05), Newport Beach, CA, April 21-23. pp. 531-535.